

## Synthesis and Self-Assembly of D and L Type Peptides

Alyssa Monohon and Katherine Galgozy  
Department of Chemistry  
Gannon University  
109 University Square  
Erie, PA, 16541

Faculty Advisor: Dr. Ria J. Betush

### Abstract

Self-assembling peptides are of great interest due to their applications in controlled release drug delivery, vaccine development, tissue engineering, and wound healing. Designed peptides with alternating polar and nonpolar amino acid side chains tend to form  $\beta$ -sheets in water. These further pack to form a bilayer and extend into fibrils. The peptide Ac-(FKFE)<sub>2</sub>-NH<sub>2</sub> is an example of one of these  $\beta$ -sheet forming peptides, which has been well characterized in all L and all D forms. This current research examines the influence of changes to length and chirality on the self-assembly properties and fibril morphology. The first set of peptides combines L and D amino acids within a single peptide strand using sequences Ac-FKfefeFE-NH<sub>2</sub>, Ac-fkFEFKfe-NH<sub>2</sub>, and Ac-fkfeFKFE-NH<sub>2</sub>, where uppercase are L, and lowercase are D residues. The second set of peptides examines chain length using L and D Ac-FKFEFKFEF-NH<sub>2</sub>, with an additional C-terminal F. These modified sequences were synthesized using Fmoc techniques with HBTU and HOBT, on rink amide resin. Upon completion of amino acid coupling, the N-terminus was acetylated and the peptide was cleaved using TFA. Methods for purification were developed and completed using high performance liquid chromatography (HPLC). Concentration curves were acquired from a sequence of serial dilutions run in triplicate and confirmed by amino acid analysis. Purified peptides were assembled in water and self-assembly of all sequences was confirmed by transmission electron microscopy (TEM), circular dichroism (CD), and Fourier transform infrared spectroscopy (FTIR). Continuing work is being conducted to synthesize additional peptides with <sup>13</sup>C labels for FTIR study. The addition of these labels to the peptide strands will provide interstrand interaction data via the amide stretch that may help us better understand  $\beta$ -sheet packing of both sets of peptides.

**Keywords:** Peptide, Self-Assembly, FTIR

### 1. Introduction

Self-assembling peptides have become of increasing interest due to their biomaterial and biomedical applications. The assembled materials have found application as cell scaffolds, delivery agents, immune response therapies, and in tissue engineering.<sup>1-8</sup> One well-studied subcategory is  $\beta$ -sheet self-assembling peptides, due in part to their high propensity to self-assemble in aqueous environments. Study of amphipathic  $\beta$ -sheet peptides originated with the EAK16 peptide, derived from the yeast Zuotin protein.<sup>9-10</sup> This peptide and many derived from its sequence contain alternating hydrophobic and hydrophilic amino acids, which enforces a  $\beta$ -strand structure that places the hydrophobic amino acids all to one side of the strand and the hydrophilic amino acids to the other side. As exemplified by the Ac-(FKFE)<sub>2</sub>-NH<sub>2</sub> peptide in Figure 1, these amphipathic peptides pack next to each other, creating a  $\beta$ -sheet, and further laminate two  $\beta$ -sheets, creating a bilayer. This allows the hydrophobic faces of both sheets to be buried inside and the hydrophilic sides exposed to water, creating the solubility of the self-assembled peptide fibrils.<sup>11-13</sup>  $\beta$ -sheet fibrils are held together by noncovalent interactions and modifications have been made to these peptides to alter their mechanical properties and self-assembling propensity.<sup>14-18</sup>

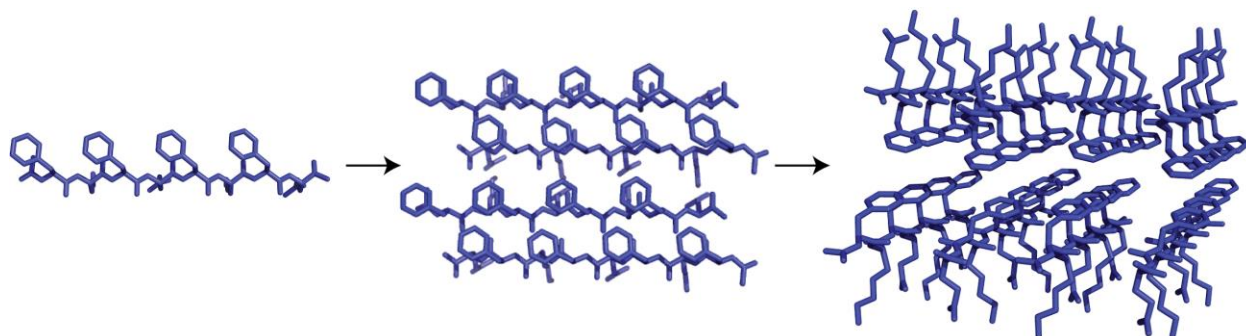


Figure 1. Ac-FKFEFKFE-NH<sub>2</sub> from  $\beta$ -strand to  $\beta$ -sheet to  $\beta$ -sheet bilayer.

Proteins and peptides studied are often composed of L amino acids, the naturally occurring enantiomers found in the human body. However, D-amino acid peptides have been increasingly studied to understand their properties and utility. They have been shown to have increased proteolytic stability over their L-conformers, which increases the time the peptide is active in the body due to their resistance to enzymes designed to cleave L-proteins.<sup>19-21</sup> The increased proteolytic stability has been shown not only for all D-peptides, but also C- and N-terminal D-substituted peptides, where the middle section remains L- to maintain function.<sup>22-23</sup> Self-assembling  $\beta$ -sheet peptides synthesized with all D-amino acids are found to have similar mechanical characteristics to the L- versions of the same peptide, though with different interactions towards biological systems.<sup>24-27</sup> Peptide length was moderately altered to Ac-FKFEFKFE-NH<sub>2</sub>, adding one C-terminal phenylalanine in both all L and all D amino acids. These peptides were synthesized and purified and are awaiting further experimentation to examine their self-assembly properties.

Mixing D- and L-amino acids into a single peptide strand has yielded mixed results. Alternating D- and L-amino acids in a single strand in cyclic form has resulted in the formation of nanotubes, but alternating amino acids in the linear peptide EAK16 has resulted in breaking  $\beta$ -sheet structure.<sup>28-29</sup> In the first set of peptides, a conservative approach to mixing D- and L-amino acids in a single strand was used to examine peptides with longer blocks of D- and L-amino acids using the overall sequence Ac-(FKFE)<sub>2</sub>-NH<sub>2</sub> (Figure 2A). This sequence, a derivative of Zhang's EAK16 peptide, has been well studied in both D and L forms. It has been shown to quickly form  $\beta$ -sheet fibrils with a helical twist corresponding to the chirality of the amino acids, right-handed for the D-peptide and left-handed for the L-peptide, that flatten into long fibrils ~8.2 nm wide after several hours.<sup>13,25,30-31</sup>

The peptide sequence was modified to the three sequences Ac-FKfEfKFE-NH<sub>2</sub>, Ac-fkFEFKfe-NH<sub>2</sub>, and Ac-fkfeFKFE-NH<sub>2</sub> where the uppercase letters are L-amino acids and the lowercase letters are D-amino acids. Ac-FKfEfKFE-NH<sub>2</sub> has been the most extensively studied thus far and is proposed to have similar properties to the parent Ac-(FKFE)<sub>2</sub>-NH<sub>2</sub> while allowing for possible new morphologies and increased proteolytic stability. The Ac-FKfEfKFE-NH<sub>2</sub> peptide sequence has two changes in chirality in the peptide strand, so the peptide backbone would have to twist to still allow formation of a hydrophobic and hydrophilic face, a problem not faced by Ac-(FKFE)<sub>2</sub>-NH<sub>2</sub> (Figure 2B).

The Ac-FKfEfKFE-NH<sub>2</sub> peptide was synthesized, purified, and examined by FTIR for self-assembly propensity. The FTIR experiments have shown that while the peptide forms  $\beta$ -sheets, it remains partially unassembled immediately after assembly. The two changes to chirality with D- and L- modifications within a single strand were shown to lower, but not eliminate  $\beta$ -sheet assembly of the peptides. The twist of the peptides that would be required to form a  $\beta$ -strand may minimize  $\beta$ -sheet formation. Additional labeled amino acid studies will be conducted to better understand how the individual peptide strands are interacting.

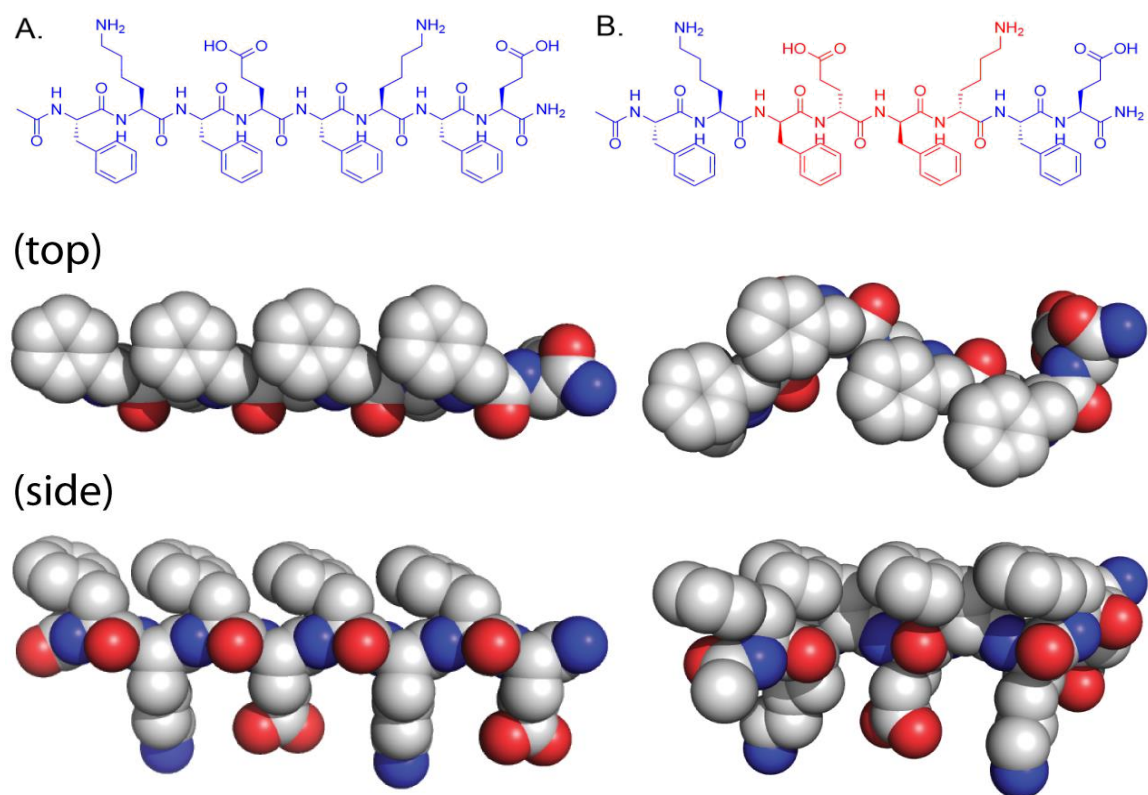


Figure 2. Chemdraw images of (A) all L Ac-(FKFE)<sub>2</sub>-NH<sub>2</sub> and (B) Ac-FKfefeFE-NH<sub>2</sub>, blue represents L-amino acids and red represents D-amino acids. Underneath, space-filling models rotated at the amide bond to maintain a hydrophobic and hydrophilic face.

## 2. Methodology

### 2.1 Peptide Synthesis

Peptides were synthesized on rink amide resin (Advanced ChemTech, 100-200 mesh, 0.3 mmol g<sup>-1</sup>) utilizing standard solid-phase Fmoc deprotection and HOBt-HBTU activation loading methods. The peptides were acetylated following final N-terminal deprotection. A mixture of trifluoroacetic acid (TFA), triisopropylsilane, and water (95:2.5:2.5 by volume) was used to cleave the peptide from resin and for removal of protecting groups at room temperature twice for one hour each. The cleaved peptide was partially evaporated in vacuo and 40% acetonitrile in water was added. The sample was frozen and lyophilized. The crude peptide powder was dissolved in DMSO and purified by preparatory high performance liquid chromatography (HPLC).

### 2.2 Purification

The cleaved peptides were purified by HPLC using a reverse phase C18 column (Phenomenex, Gemini 10 μm, 21.2 x 250 mm) on a Shimadzu LC-20AT HPLC system. A gradient of water and acetonitrile with 0.1% TFA at 10 mL min<sup>-1</sup> was used and the eluent was monitored by UV absorbance at 215 and 254 nm. Fractions were collected and lyophilized once their purity was confirmed by analytical HPLC performed using an RP-C18 column (Phenomenex, Gemini, 5 μm, 4.6 x 250 mm) and MALDI-TOF mass spectroscopy. The analytical HPLC method ran for 2 minutes at 5% acetonitrile, increased to 95% over 12 minutes, held for 5 minutes, and over 12 minutes, lowered back to 5% and held to reequilibrate the column.

## 2.3 Peptide Self-Assembly

Peptide self-assembly was assessed in water once proper concentrations were determined. Standard concentration curves were constructed by analytical HPLC and absolute concentrations for each curve were determined by amino acid analysis (UC Davis, Proteomics Core). Peptide concentrations were determined by correlation to the standard curves and prepared into 1.0 mM aliquots in 60/39.9 D<sub>2</sub>O/D<sub>3</sub>-acetonitrile with 0.1% either TFA or DCI, frozen, and lyophilized. This was repeated twice to ensure complete exchange of the deuterium and, in some cases, TFA remaining from purification to DCI. The lyophilized peptides were dissolved in D<sub>2</sub>O and vortexed for one minute to obtain optically clear, homogenous solutions. Peptide solutions were analyzed immediately upon vortexing.

## 2.4 Fourier Transform Infrared Spectroscopy (FTIR)

FTIR spectra were obtained with a Perkin Elmer Spectrum 2 FT-IR spectrophotometer. All peptides were solubilized in D<sub>2</sub>O in place of H<sub>2</sub>O and prepared as in peptide self-assembly. Absorbance spectrums were obtained from 600 to 4000 cm<sup>-1</sup> with a 2 cm<sup>-1</sup> resolution, Happ-Ganzel Apodization, and 512 scans with CaF<sub>2</sub> salt plates (25 x 4 mm, International Crystal Labs).

## 3. Data

### 3.1 Synthesis and Purification

Solid-phase synthesis of peptides necessitates purification to remove incomplete sequences from the desired peptide. This was completed using preparatory HPLC methods described in 2.2. The purified peptide was rerun using an analytical HPLC column to determine purity and aid in the formation of a concentration curve.

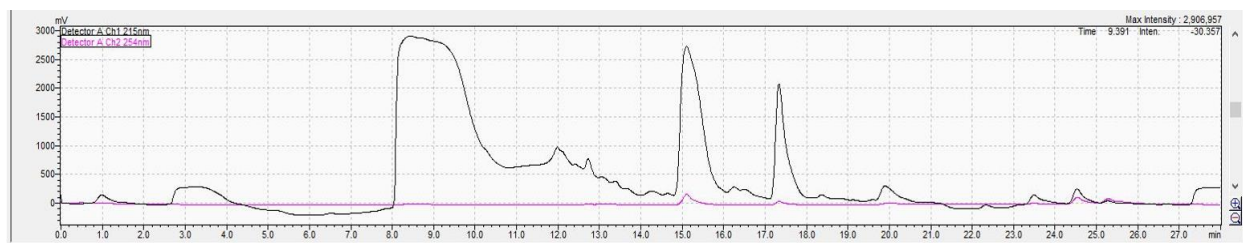


Figure 3. Crude Ac-(FKFE)<sub>2</sub>-NH<sub>2</sub> peptide on preparatory HPLC column for purification.

Figure 3 shows the crude peptide after it is synthesized, lyophilized, and dissolved in DMSO. The peak at 15.0 minutes represents Ac-(FKFE)<sub>2</sub>-NH<sub>2</sub> and was collected to yield pure peptide. A gradient of increasing acetonitrile was used (reverse-phase HPLC) and the peptide eluted at approximately 35% acetonitrile, affected largely by the nonpolar phenylalanine. The all L sequence Ac-(FKFE)<sub>2</sub>-NH<sub>2</sub> was synthesized and purified, as were the three chiral modifications, Ac-FKfefeNH<sub>2</sub>, Ac-fkFEFKfeNH<sub>2</sub>, and Ac-fkfeFKFE-NH<sub>2</sub>, and the two length modification sequences, L and D Ac-FKFEFKFE-NH<sub>2</sub>.

### 3.2 Concentration curve

Pure Ac-(FKFE)<sub>2</sub>-NH<sub>2</sub> peptide was run on an analytical column on the HPLC to verify purity (Figure 4). The absence of additional peaks, coupled with MALDI-MS and amino acid analysis, confirmed that this was the desired peptide. The lyophilizer was used to remove the solvent from the solution instead of rotary evaporation to avoid assembly as concentration increased by the removal of the liquid solvent. Freeze-drying allows the solvent to skip the liquid phase and sublime instead.

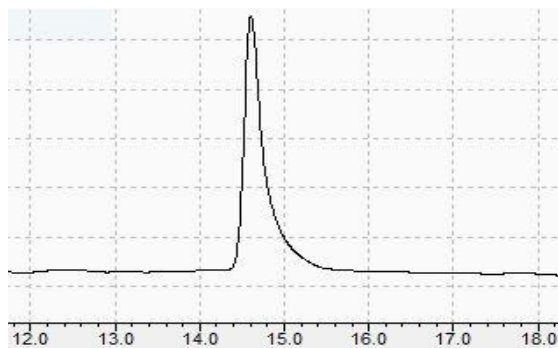


Figure 4. Analytical HPLC trace of pure Ac-(FKFE)<sub>2</sub>-NH<sub>2</sub>.

The amount of peptide needed to be quantified in order to utilize the peptide for future experimentation. Absolution concentration was determined by samples sent to UC Davis for amino acid analysis in combination with the generation of a concentration curve by analytical HPLC. To generate the concentration curve, lyophilized purified Ac-(FKFE)<sub>2</sub>-NH<sub>2</sub> was mixed with 50% acetonitrile in water and the solution was vortexed for 1 minute to ensure proper mixing. A set of four serial dilutions was completed and a portion of the highest concentration was sent for amino acid analysis. The samples were run from lowest to highest concentration in triplicate, averaged, and plotted. This information allowed the creation of a concentration curve from the best fit curve (Figure 5). Equation (1) was generated with Y representing nmol of sample and X being the area of the peak done by integration in HPLC data analysis.

$$Y = (5.98 \times 10^{-7}) \times X \tag{1}$$

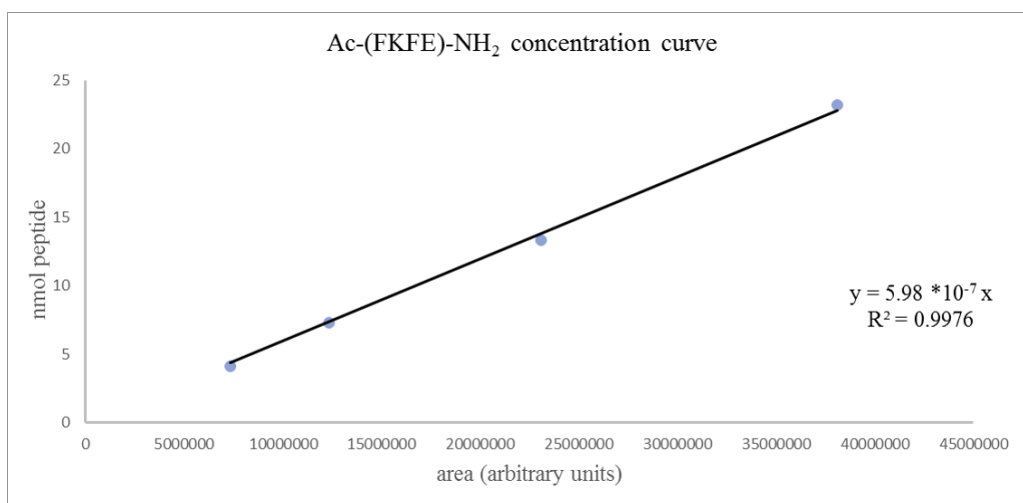


Figure 5. Concentration curve for Ac-(FKFE)<sub>2</sub>-NH<sub>2</sub>.

Using the constructed concentration curve, samples were prepared for FTIR that would yield a concentration of 1.0 mM upon the final addition of D<sub>2</sub>O. The concentration curve generated for Ac-(FKFE)<sub>2</sub>-NH<sub>2</sub> was able to be utilized for all of the eight amino acid sequences as the changes in chirality between L and D amino acids do not influence the integration of the peak. The required amount of purified peptide was added to 200 μL of 60 D<sub>2</sub>O/ 39.9 D<sub>3</sub>-CH<sub>3</sub>CN/ 0.1 DCI or TFA and lyophilized. This was repeated and the twice lyophilized peptide was sealed in a desiccator prior to the FTIR study.

### 3.3 Fourier Transform Infrared Spectroscopy (FTIR)

FTIR spectra were obtained for Ac-(FKFE)<sub>2</sub>-NH<sub>2</sub> and Ac-FKf<sub>2</sub>FE-NH<sub>2</sub> peptides at 1.0 mM concentration, prepared as stated in Section 2.3. To reduce interference from water, which can overlap in the relevant region of the IR, D<sub>2</sub>O was utilized instead of H<sub>2</sub>O. With peptides in D<sub>2</sub>O which are expected to form  $\beta$ -sheet structures, a peak from 1620-1630 cm<sup>-1</sup> indicates  $\beta$ -sheet formation, a small peak at 1690 cm<sup>-1</sup> indicates that it is an antiparallel  $\beta$ -sheet; a peak around 1646 cm<sup>-1</sup> would indicate that the peptide remained unstructured.<sup>32</sup> Additionally, 0.1% acid, either TFA or DCI, was maintained throughout lyophilization to ensure a consistent pH. TFA is known to have a peak near 1675 cm<sup>-1</sup>. Initial FTIR studies of each peptide were conducted without exchanging the TFA to determine if the small amount of residual TFA would affect the spectra in pure D<sub>2</sub>O. For the peptide Ac-(FKFE)<sub>2</sub>-NH<sub>2</sub> with TFA, a peak is seen at 1624 cm<sup>-1</sup>, indicative of a  $\beta$ -sheet structure, but a large peak at 1676 cm<sup>-1</sup> was present, indicating absorbance from the TFA. This peak also covers the known antiparallel peak of Ac-(FKFE)<sub>2</sub>-NH<sub>2</sub> at 1686 cm<sup>-1</sup> (Figure 6A, top line). A similar TFA peak is observed with Ac-FKf<sub>2</sub>FE-NH<sub>2</sub> (Figure 6B, top line).

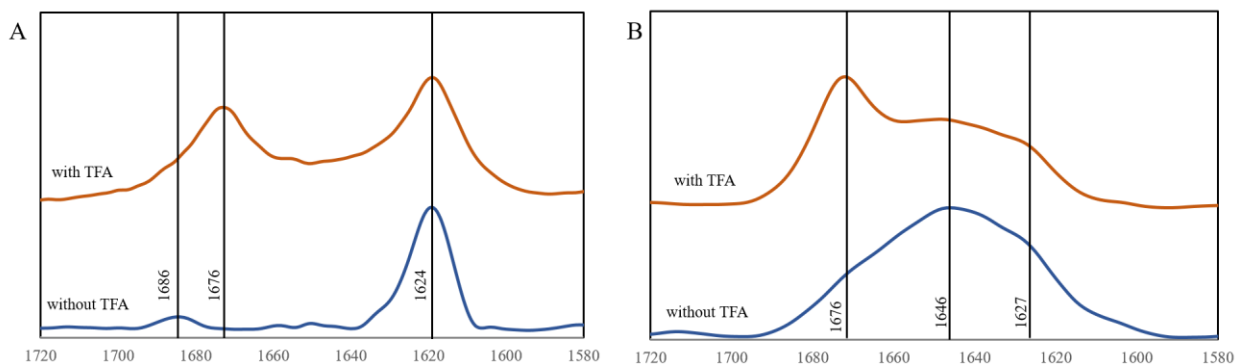


Figure 6. A. FTIR absorbance of Ac-(FKFE)<sub>2</sub>-NH<sub>2</sub> and B. Ac-FKf<sub>2</sub>FE-NH<sub>2</sub> at 1.0 mM concentration with TFA (red lines) and without TFA (blue lines).

The TFA peak overwhelms portions of the relevant peaks, so all further FTIR experiments were conducted using 0.1% DCI to exchange with the TFA. Figure 6A, bottom line shows Ac-(FKFE)<sub>2</sub>-NH<sub>2</sub> immediately after 1 minute of vortexing, with visible peaks at 1624 and 1686 cm<sup>-1</sup>. These points of assembly indicate an antiparallel  $\beta$ -sheet configuration consistent with the literature.<sup>25</sup> Figure 6B, bottom line, shows Ac-FKf<sub>2</sub>FE-NH<sub>2</sub> immediately after 1 minute of vortexing, and a small peak near 1627 cm<sup>-1</sup> as well as a larger peak at 1646 cm<sup>-1</sup>. While the smaller peak indicates some  $\beta$ -sheet self-assembly, the peak at 1646 cm<sup>-1</sup> signifies incomplete assembly. Preliminary results from collaborators at the University of Rochester is inconclusive on self-assembly by circular dichroism (CD) as the presence of D and L amino acids convolutes the signal. However, transmission electron microscopy (TEM) indicates that fibril formation occurs, confirming peptide self-assembly is occurring for this peptide.

## 4. Conclusion

Ac-(FKFE)<sub>2</sub>-NH<sub>2</sub> and Ac-FKf<sub>2</sub>FE-NH<sub>2</sub> were synthesized and purified in order to study the self-assembling propensities from the amide stretch present on FTIR spectra. Proper study necessitated the construction of a concentration curve for Ac-(FKFE)<sub>2</sub>-NH<sub>2</sub>. For optimal FTIR data by minimizing interferences from TFA and water, deuterium exchanges with D<sub>2</sub>O and DCI were completed. When comparing the FTIR spectra for Ac-(FKFE)<sub>2</sub>-NH<sub>2</sub> and Ac-FKf<sub>2</sub>FE-NH<sub>2</sub>, the Ac-(FKFE)<sub>2</sub>-NH<sub>2</sub> spectrum displays more sharp peaks at 1624 and 1686 cm<sup>-1</sup>, indicating antiparallel  $\beta$ -sheet formation. However, the Ac-FKf<sub>2</sub>FE-NH<sub>2</sub> FTIR spectrum displays a peak at 1627 cm<sup>-1</sup> and a larger broad peak at 1646 cm<sup>-1</sup>, indicating poor self-assembly at 1.0 mM concentration. This is most likely due to the altered spatial configuration from the two points of chirality change. These two changes could hinder the formation of the hydrophobic and hydrophilic faces in a  $\beta$ -sheet configuration.

## 5. Future Work

FTIR spectra will be obtained for the Ac-fkFEFKfe-NH<sub>2</sub> and Ac-fkfeFKFE-NH<sub>2</sub> sequences, which have been synthesized and purified. These experiments will expand the understanding of how modifications and the number of modifications to the chirality of the peptide backbone affects self-assembly. The current Ac-FKfekFE-NH<sub>2</sub> sequence will be synthesized with <sup>13</sup>C labeled amino acids to understand the interactions between peptide strands. It is expected that <sup>13</sup>C labeled carbonyl carbon of the isotope-edited peptides will have a lower wavenumber on the FTIR spectrum. The distance the amide stretch shifts will provide insight on these peptide interactions. Additionally, L and D Ac-FKFEFKFE-NH<sub>2</sub> have been synthesized and purified to study the effect of chain length on peptide self-assembly. Similar methodology will be used to obtain new concentration curves and FTIR data for these peptides.

## 6. Acknowledgements

We would like to thank Gannon University's Department of Chemistry and Biochemistry and the Gannon University Faculty Research Grant for their financial support. We also thank the Nilsson lab at the University of Rochester for their contributions with performing MALDI-MS, CD, and TEM.

## 7. References

1. Park, S. E.; Sajid, M. I.; Parang, K.; Tiwari, R. K., Cyclic Cell-Penetrating Peptides as Efficient Intracellular Drug Delivery Tools. *Mol. Pharm.* **2019**, *16* (9), 3727-3743.
2. Carlini, A. S.; Gaetani, R.; Braden, R. L.; Luo, C.; Christman, K. L.; Gianneschi, N. C., Enzyme-responsive progelator cyclic peptides for minimally invasive delivery to the heart post-myocardial infarction. *Nat. Commun.* **2019**, *10* (1), 1735.
3. Li, I. C.; Moore, A. N.; Hartgerink, J. D., "Missing Tooth" Multidomain Peptide Nanofibers for Delivery of Small Molecule Drugs. *Biomacromolecules* **2016**, *17* (6), 2087-2095.
4. Branco, M. C.; Schneider, J. P., Self-assembling materials for therapeutic delivery. *Acta Biomater.* **2009**, *5*, 817-831.
5. De Leon-Rodriguez, L. M.; Park, Y.-E.; Naot, D.; Musson, D. S.; Cornish, J.; Brimble, M. A., Design, characterization and evaluation of  $\beta$ -hairpin peptide hydrogels as a support for osteoblast cell growth and bovine lactoferrin delivery. *RSC Adv.* **2020**, *10* (31), 18222-18230.
6. Saha, S.; Yang, X. B.; Wijayathunga, N.; Harris, S.; Feichtinger, G. A.; Davies, R. P. W.; Kirkham, J., A biomimetic self-assembling peptide promotes bone regeneration in vivo: A rat cranial defect study. *Bone* **2019**, *127*, 602-611.
7. Raymond, D. M.; Nilsson, B. L., Multicomponent peptide assemblies. *Chem. Soc. Rev.* **2018**, *47* (10), 3659-3720.
8. Cheng, T.-Y.; Chen, M.-H.; Chang, W.-H.; Huang, M.-Y.; Wang, T.-W., Neural stem cells encapsulated in a functionalized self-assembling peptide hydrogel for brain tissue engineering. *Biomaterials* **2013**, *34* (8), 2005-2016.
9. Zhang, S.; Holmes, T.; Lockshin, C.; Rich, A., Spontaneous assembly of a self-complementary oligopeptide to form a stable macroscopic membrane. *Proc. Natl. Acad. Sci. U. S. A.* **1993**, *90* (8), 3334-8.
10. Zhang, S.; Lockshin, C.; Cook, R.; Rich, A., Unusually stable beta-sheet formation in an ionic self-complementary oligopeptide. *Biopolymers* **1994**, *34* (5), 663-72.
11. De Leon Rodriguez, L. M.; Hemar, Y.; Cornish, J.; Brimble, M. A., Structure-mechanical property correlations of hydrogel forming [small beta]-sheet peptides. *Chem. Soc. Rev.* **2016**, *45* (17), 4797-4824
12. Sun, Y.; Zhang, Y.; Tian, L.; Zhao, Y.; Wu, D.; Xue, W.; Ramakrishna, S.; Wu, W.; He, L., Self-assembly behaviors of molecular designer functional RADA16-I peptides: influence of motifs, pH, and assembly time. *Biomed. Mater.* **2016**, *12* (1), 015007.
13. Marini, D. M.; Hwang, W.; Lauffenburger, D. A.; Zhang, S.; Kamm, R. D., Left-Handed Helical Ribbon Intermediates in the Self-Assembly of a beta-Sheet Peptide. *Nano Lett.* **2002**, *2* (4), 295-299.

14. Weber, R.; McCullagh, M., The Role of Hydrophobicity in the Stability and pH-Switchability of (RXDX)<sub>4</sub> and Coumarin–(RXDX)<sub>4</sub> Conjugate  $\beta$ -Sheets. *J. Phys. Chem. B* **2020**, *124* (9), 1723-1732.
15. Sinthuvanich, C.; Nagy-Smith, K. J.; Walsh, S. T. R.; Schneider, J. P., Triggered Formation of Anionic Hydrogels from Self-Assembling Acidic Peptide Amphiphiles. *Macromolecules* **2017**, *50* (15), 5643-5651.
16. Wen, Y.; Waltman, A.; Han, H.; Collier, J. H., Switching the Immunogenicity of Peptide Assemblies Using Surface Properties. *ACS Nano* **2016**, *10* (10), 9274-9286.
17. Betush RJ, Urban JM, Nilsson BL. Balancing hydrophobicity and sequence pattern to influence self assembly of amphipathic peptides. *Peptide Science*. **2018**;110: e23099
18. Maude, S.; Ingham, E.; Aggeli, A., Biomimetic self-assembling peptides as scaffolds for soft tissue engineering. *Nanomedicine* **2013**, *8* (5), 823-847.
19. Swanekamp, R.J.; Welch, J.J.; Nilsson, B.L. Proteolytic stability of amphipathic peptide hydrogels composed of self-assembled pleated beta-sheet or coassembled rippled beta-sheet fibrils. *Chem. Commun.* **2014**, *50*, 10133–10136.
20. Hong, S. Y.; Oh, J. E.; Lee, K.-H., Effect of d-amino acid substitution on the stability, the secondary structure, and the activity of membrane-active peptide. *Biochem. Pharmacol.* **1999**, *58* (11), 1775-1780.
21. Hyland, L. L.; Twomey, J. D.; Vogel, S.; Hsieh, A. H.; Yu, Y. B., Enhancing Biocompatibility of D-Oligopeptide Hydrogels by Negative Charges. *Biomacromolecules* **2013**, *14* (2), 406-412.
22. Oyston, P. C. F.; Fox, M. A.; Richards, S. J.; Clark, G. C., Novel peptide therapeutics for treatment of infections. *J. Med. Microbiol.* **2009**, *58* (8), 977-987.
23. Tugyi, R.; Uray, K.; Iván, D.; Fellingner, E.; Perkins, A.; Hudecz, F., Partial -amino acid substitution: Improved enzymatic stability and preserved Ab recognition of a MUC2 epitope peptide. *Proc. Natl. Acad. Sci. U. S. A.* **2005**, *102* (2), 413.
24. Urban, J. M.; Ho, J.; Piester, G.; Fu, R.; Nilsson, B. L., Rippled beta-Sheet Formation by an Amyloid-beta Fragment Indicates Expanded Scope of Sequence Space for Enantiomeric beta-Sheet Peptide Coassembly. *Molecules* **2019**, *24* (10).
25. Swanekamp, R. J.; DiMaio, J. T.; Bowerman, C. J.; Nilsson, B. L., Coassembly of enantiomeric amphipathic peptides into amyloid-inspired rippled beta-sheet fibrils. *J. Am. Chem. Soc.* **2012**, *134* (12), 5556-9.
26. Nagy-Smith, K.; Beltramo, P. J.; Moore, E.; Tycko, R.; Furst, E. M.; Schneider, J. P., Molecular, Local, and Network-Level Basis for the Enhanced Stiffness of Hydrogel Networks Formed from Coassembled Racemic Peptides: Predictions from Pauling and Corey. *ACS Cent. Sci.* **2017**, *3* (6), 586-597.
27. Luo, Z.; Zhao, X.; Zhang, S., Self-Organization of a Chiral D-EAK16 Designer Peptide into a 3D Nanofiber Scaffold. *Macromol. Biosci.* **2008**, *8* (8), 785-791.
28. Ghadiri, M. R.; Granja, J. R.; Milligan, R. A.; McRee, D. E.; Khazanovich, N., Self-assembling organic nanotubes based on a cyclic peptide architecture. *Nature* **1993**, *366* (6453), 324-327.
29. Luo, Z.; Zhang, S., Designer nanomaterials using chiral self-assembling peptide systems and their emerging benefit for society. *Chem. Soc. Rev.* **2012**, *41* (13), 4736-4754.
30. Bowerman, C. J.; Nilsson, B. L., Self-assembly of amphipathic beta-sheet peptides: insights and applications. *Biopolymers* **2012**, *98* (3), 169-84.
31. Hwang, W.; Marini, D. M.; Kamm, R. D.; Zhang, S., Supramolecular structure of helical ribbons self-assembled from a beta-sheet peptide. *J. Chem. Phys.* **2003**, *118* (1), 389-397.
32. Barth, A., Infrared spectroscopy of proteins. *Biochim. Biophys. Acta Bioenerg.* **2007**, *1767* (9), 1073-1101.